

Appendix D

Spatial and Temporal Variability of Surface Water pCO₂ and Sampling Strategies

Colm Sweeney, Taro Takahashi, and Anand Gnanadesikan
in collaboration with
Rik Wanninkhof, Richard A. Feely, Gernot Friedrich, Francisco Chaves,
Nicolas Bates, Jon Olafsson, and Jorge Sarmiento

D.1 Introduction

The difference between the partial pressure of CO₂ (pCO₂) in surface ocean water and that in the overlying air represents the thermodynamic driving force for the CO₂ transfer across the sea surface. The direction of the net transfer flux of CO₂ is governed by the pCO₂ differences, and the magnitude of the flux may be expressed as a product of the pCO₂ difference and the gas transfer coefficient. Presently the only practical means for estimating the net sea-air CO₂ flux over the global oceans is a combination of the sea-air pCO₂ difference and the CO₂ gas transfer coefficient. Although an eddy correlation method aboard a ship at sea (Wanninkhof and McGillis, 1999) was successfully deployed over the North Atlantic during the recent GASEX-99 program, its applications is still limited. The objective of this report is (1) to analyze the spatial and temporal variability of surface water pCO₂ based on the available field observations, and (2) to recommend sampling frequencies in space and time needed for estimating net sea-air CO₂ flux in regional scales with a specified uncertainty and a known sea-air gas transfer coefficient on wind speed. It should be noted that the sampling frequencies needed for investigation of governing processes such as photosynthesis and upwelling are not addressed in this report.

D.2 General Background

Over the global oceans, the pCO₂ in surface ocean water is known to vary geographically and seasonally over a wide range between about 150 μatm and 500 μatm , or about 50% below and above the 2001 atmospheric pCO₂ level of about 360 μatm (or 370 ppm in CO₂ mole fraction concentration in dry air).

D.2.1 Factors that determine variability of pCO₂

The pCO₂ in mixed layer waters, which exchange CO₂ directly with the atmosphere, is affected by temperature, the total CO₂ concentration, and the alkalinity. While the water temperature is regulated by physical processes

(i.e., solar energy input, sea-air heat exchanges, and mixed layer thickness), the latter two are primarily controlled by biological processes (i.e., photosynthesis and respiration) and by upwelling of subsurface waters enriched in CO_2 and nutrients. The $p\text{CO}_2$ in surface ocean waters doubles for every 16°C temperature increase. For a parcel of seawater with constant chemical composition, $p\text{CO}_2$ would increase by a factor of 4 when it is warmed from polar water temperatures of about -1.9°C to equatorial water temperatures of about 30°C . However, the total CO_2 concentration in surface waters ranges from about $2150 \mu\text{mol}/\text{kg}$ in polar waters to $1850 \mu\text{mol}/\text{kg}$ in equatorial waters. If a global mean Revelle factor of 10 is used, this reduction of TCO_2 should cause a reduction of $p\text{CO}_2$ by a factor of 4.5. Thus, on a global scale, the effect of biology and upwelling on surface water $p\text{CO}_2$ is similar in magnitude but often opposite in direction to the temperature effect. The increasing effect on seawater $p\text{CO}_2$ of summer warming of water is commonly opposed by the lowering effect of photosynthesis during summer months. The decreasing effect on $p\text{CO}_2$ of winter cooling of water is counteracted by the increase in the total CO_2 concentration caused by winter convective mixing of deep waters rich in CO_2 . It is therefore the interactions of the three major effects (i.e., temperature, upwelling, and biological utilization of CO_2) that determine the annual mean $p\text{CO}_2$ and variability about the mean in space and time.

D.2.2 Variability of surface water $p\text{CO}_2$

The spatial variability of the surface water $p\text{CO}_2$ is demonstrated in Fig. D-1 using about 700,000 $p\text{CO}_2$ observations made in the past 40 years by Takahashi *et al.* (1999). The standard deviation of observed $p\text{CO}_2$ values in each $4^\circ \times 5^\circ$ pixel was computed for each month, and the mean of the monthly standard deviation values have been plotted in color. The white areas indicate the pixels with no observations. The map, therefore, shows the magnitude of mean $p\text{CO}_2$ variability over the period of a month within each pixel area. It should be noted that some pixels have observations in all 12 months, whereas some pixels have observations only in one or more months. Small spatial variability (magenta-blue) is found mainly in the subtropical oceans, whereas large variability (green-yellow-orange) is found in the equatorial Pacific and the high-latitude oceans of both hemispheres, where concentrations of nutrients are large and productivity is high. The large $p\text{CO}_2$ variability in these areas may be attributed to mesoscale variability in biology as well as physical features such as eddies and internal waves.

Large spatial variability also has been observed in the areas affected by major western boundary current systems (Gulf Stream, Labrador Current, Brazil-Malvinas Confluence areas, Kuroshio, and Oyashio), along which eddies and filaments are formed. *Sampling strategies for surface water $p\text{CO}_2$ must be formulated by taking these areas of large spatial variability into consideration.*

The seasonal variability of surface water $p\text{CO}_2$ varies geographically and has a peak-to-peak amplitude which is as large as $280 \mu\text{atm}$ in some regions. Seasonal amplitudes exceeding $100 \mu\text{atm}$ have been observed in the

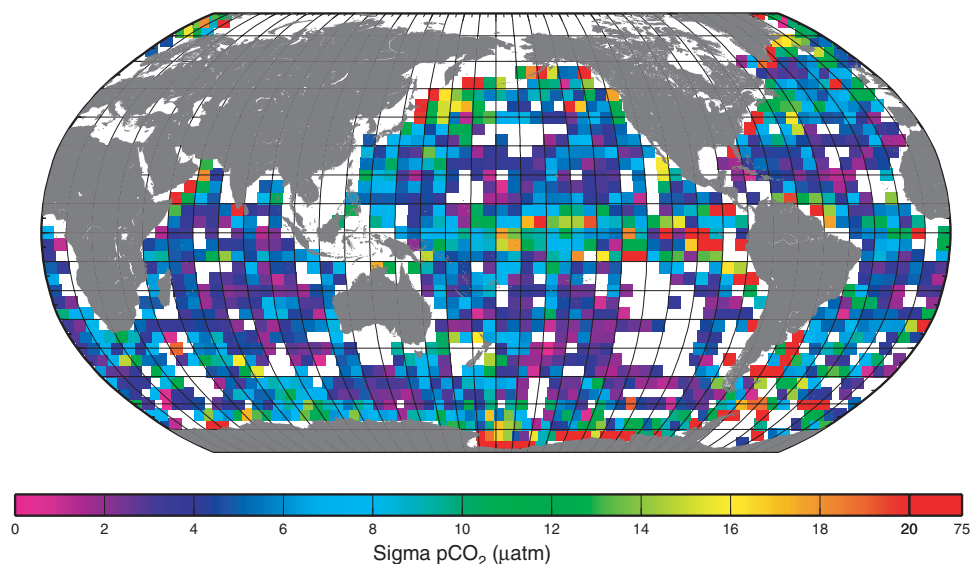
Average of Monthly Standard Deviations of pCO₂ in 4° × 5° Pixels

Figure D-1: Spatial variability of the surface water pCO₂ represented by the standard deviation of observed pCO₂ values in a month.

northwestern Arabian Sea, the northwestern subarctic Pacific, the subarctic North Atlantic, the eastern Sargasso Sea (Bermuda area), and the Ross and Weddell Seas, Antarctica. In subtropical gyre areas (e.g., Bermuda area), the seasonal variation in surface water pCO₂ is primarily driven by seasonal temperature changes, and hence pCO₂ is highest during summer and lowest in winter. On the other hand, in subpolar and polar oceans, the pCO₂ is highest during winter due to upwelling and is lowest during summer due to photosynthesis. Therefore, seasonal changes in high latitude areas are about 6 months out of phase from those in subtropical areas. Transition areas in between these two regimes (e.g., Weather Station “P”) exhibit small seasonal amplitudes as a result of interactions of these out of phase forcings. The seasonal and temporal variability of surface water pCO₂ in specific areas will be discussed in Section 4.

D.3 Regional CO₂ Flux and Sea-Air pCO₂ Difference

The monthly distributions of the sea-air pCO₂ difference over the global oceans for a reference year 1995 have been estimated using about 700,000 pCO₂ measurements made over the past 40 years. The methods for data corrections and interpolation used have been described in Takahashi *et al.* (1997, 1999). The monthly distribution maps produced represent a climatological mean for non-El Niño conditions with 4° × 5° spatial resolution. The net flux values for the global oceans and various oceanic regions have been estimated on the basis of the sea-air pCO₂ difference maps and the depen-

Table D-1: Mean annual sea-air pCO₂ difference, annual flux and the sea-air pCO₂ required for 0.1 Pg C flux*.

Ocean Regions	Average ΔpCO ₂ (μatm)	Ocean Area 10 ⁶ km ²	ΔpCO ₂ per 0.1 Pg C/yr uptake	Annual Flux Pg C/yr
Northern North Atlantic	-47.4	7.45	10.8	-0.39
Temperate North Atlantic	-9.3	23.95	5.6	-0.27
Equatorial Atlantic	+19.9	15.43	14.0	+0.13
Temperate South Atlantic	-3.1	26.08	4.4	-0.24
Polar South Atlantic	-26.4	7.10	11.3	-0.22
Northern North Pacific	-8.8	4.45	20.1	-0.02
Temperate North Pacific	-10.0	43.04	2.9	-0.47
Equatorial Pacific	+29.6	50.19	4.4	+0.64
Temperate South Pacific	-7.4	53.05	2.6	-0.36
Polar South Pacific	-9.0	17.44	4.3	-0.20
Temperate North Indian	+35.9	2.12	13.6	+0.03
Equatorial Indian	+14.0	21.05	3.7	+0.10
Temperate South Indian	-20.0	30.49	10.1	-0.57
Polar South Indian	-10.1	7.16	10.8	-0.10
Global Oceans		308.99		-1.94

*All the values are for the reference year 1995. The wind speed data of Esbensen and Kushnir (1981) and the wind speed dependence of gas transfer coefficient of Wanninkhof (1992) have been used.

dence of the CO₂ gas transfer coefficient across the sea surface on long-term wind speed, that has been formulated by Wanninkhof (1992). If the monthly mean climatological wind speeds of Esbensen and Kushnir (1981) is used, the pCO₂ data yield a global oceanic uptake of 1.94 Pg C/yr. If the 40-year mean NCEP/NCAR wind speed data are used, a global ocean uptake of 2.45 Pg C/yr is obtained. Table D-1 shows the annual mean sea-air pCO₂ difference and the net CO₂ uptake flux in various oceanographic regions, that was estimated using the wind speed data of Esbensen and Kushnir (1981).

Table D-1 shows that, in order to estimate a regional CO₂ flux within ±0.1 Pg C/yr for the major oceanic regions, the sea-air pCO₂ difference should be determined within 3 to 15 μatm. Figure D-2 shows the geographical distribution of the sea-air pCO₂ differences required for constraining flux estimates within ±0.1 Pg C/yr. Small oceanic regions such as northern North Pacific and temperate North Indian Oceans (area <4 × 10⁶ km²) are exceptions, since the net flux for these areas is much smaller than 0.1 Pg C/yr.

In order to estimate the terrestrial ecosystem uptake flux of CO₂ reliably on the basis of an inversion of atmospheric CO₂ concentration data, it has been suggested that the net CO₂ flux over each oceanic region be known within ±0.1 Pg C/yr. For this reason, the analysis presented below is focused on evaluating the error in air-sea pCO₂ difference, that corresponds to a flux error of ±0.1 Pg C/yr.

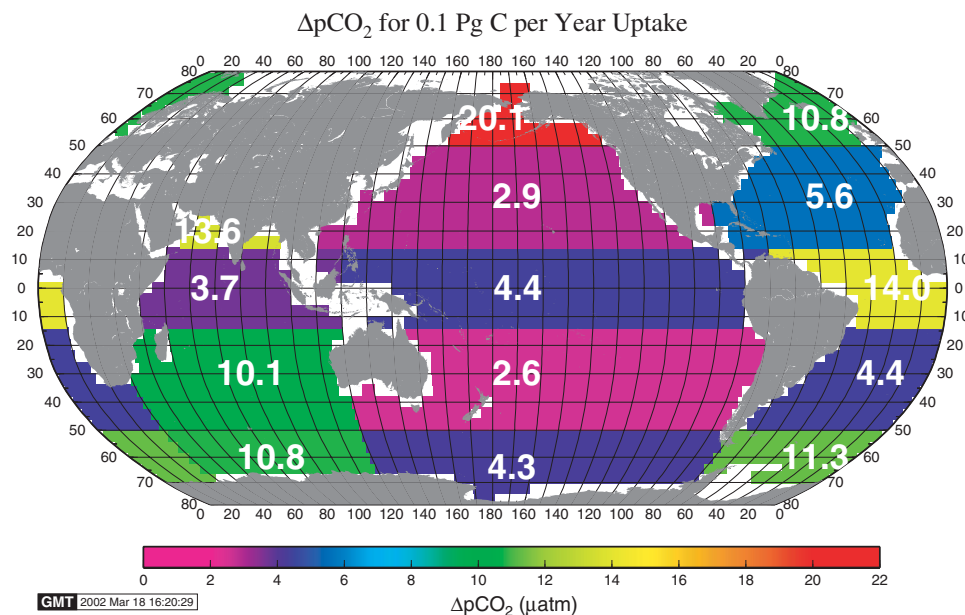


Figure D-2: Target $p\text{CO}_2$ to estimate a regional CO_2 flux within ± 0.1 Pg C/yr for the major oceanic regions from Table D-1. Polar regions cover areas between 50° and 90° (North and South), temperate regions cover areas between 14° and 50° (North and South) and equatorial regions are between 14°N and 14°S .

D.4 Temporal Variability of $p\text{CO}_2$ and Sampling Frequency

There are only a few locations where seasonal changes in surface water $p\text{CO}_2$ have been determined throughout a year. The data obtained at three locations (i.e., in the vicinity of Bermuda, Equatorial Pacific, and Weather Station “P”) will be presented and analyzed. These three locales represent the temperate gyre regime (Bermuda), the high seasonal upwelling regime (equatorial Pacific and a subarctic area north of Iceland), and the transition zone between the temperate and subarctic regimes (Weather Station “P”), respectively.

D.4.1 Temperate Gyre Regime

The temporal (seasonal) variability of $p\text{CO}_2$ and SST observed in the vicinity of the BATS Site (31°N , 64°W) are shown in Fig. D-3. Seasonal amplitude of about $100 \mu\text{atm}$ for $p\text{CO}_2$ and that of 8°C for SST are observed. The seasonal changes for $p\text{CO}_2$ appear to be in phase with those for SST. However, the observed $p\text{CO}_2$ amplitude is much smaller than that anticipated from a temperature change of 8°C , which should cause a $p\text{CO}_2$ change of about $150 \mu\text{atm}$. This difference has been attributed to the effect of biological drawdown of $p\text{CO}_2$ (about $50 \mu\text{atm}$), which is about 6 months out of phase from the effect of temperature changes (Takahashi *et al.*, submitted).

Using these data, we have computed the following two quantities. (1) Errors anticipated from measurements made at random sampling intervals,

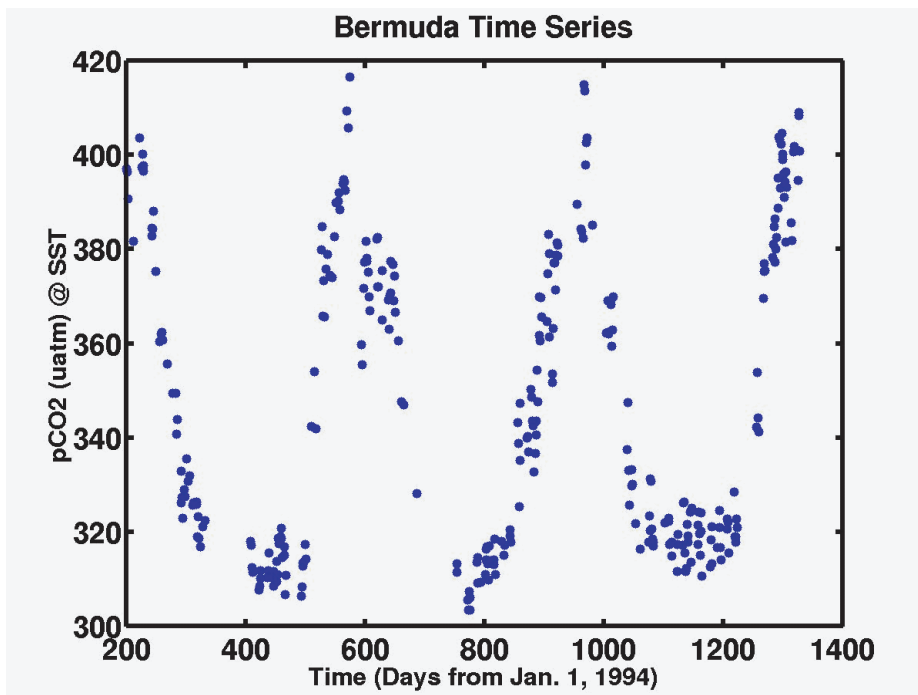


Figure D-3: Temporal variation of surface water $p\text{CO}_2$ observed in the vicinity of the BATS site (31°N , 64°W) observed in mid-1994 through early 1998 by N. Bates (BBRS).

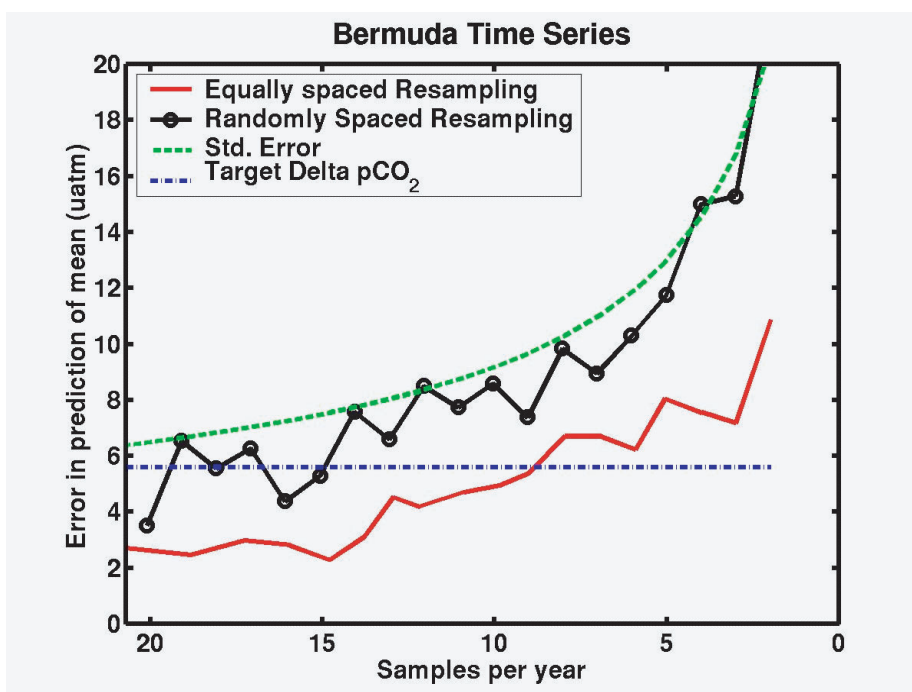


Figure D-4: Error for the annual mean value as a function of sampling frequency per year in the temperate North Atlantic in the vicinity of the BATS site. The standard error of the mean (dashed curve). Sampling with equal time intervals (solid curve). Sampling with randomly spaced time intervals (open circles and solid line). The horizontal dashed-dotted line refers to the error in $\Delta p\text{CO}_2$ needed for the estimated flux of CO_2 to the nearest 0.1 Pg C in the temperate North Atlantic.

where errors are represented by the standard error of the mean (σ/\sqrt{n}). The dashed curve in Fig. D-4 shows the anticipated error in annual mean as a function of the number of measurements made in a year. For a calendar year of 1997, 104 measurements were made in the area yielding a mean pCO₂ of 347.9 μatm with a one-sigma of 33 μatm . This curve represents simply this standard deviation (σ) value divided by the square root of the number of observations, n , per year. In order to obtain an error in the mean of 6 μatm or better (see Table D-1), measurements must be made as frequently as 30 times a year. (2) The solid curve shows errors anticipated in the mean value calculated at equally spaced sampling distances. The mean at each sampling interval was calculated by subsampling the originally over-sampled time series and using a piece-wise linear interpolation to interpolate the subsampled time series back to the original sampling interval of the time series. Thus, the mean of the subsampled time series is calculated using the same number of observations as the mean calculated from the original time series. The mean for each sampling interval was calculated a number of times by subsampling different parts of the original time series. The error in the predicted mean was computed by calculating the difference between the mean value of the linearly interpolated sub-sampled time series and the mean obtained for the entire data set. To achieve a level $\pm 6 \mu\text{atm}$ of precision in the prediction of the mean using equal sampling intervals in time nine observations are needed a year. (3) The solid line open with circles shows errors in the calculated mean if samples are taken at randomly spaced intervals in time and interpolated with a piece-wise linear fit to the original sampling intervals. As above, the error in the prediction of the mean is calculated as the difference between the mean value of the linearly interpolated sub-sampled time series and the mean obtained for the entire data set. Figure D-3 indicates that if the time series is sampled at randomly spaced intervals in time it will require at least 15 samples a year to predict the mean annual pCO₂ to within $\pm 6 \mu\text{atm}$.

The error for annual mean pCO₂ value depends not only on the total number of measurements made in a year, but also on time intervals for measurements. Considering that the temporal pattern of seasonal pCO₂ changes might be somewhat different from year to year, measurements should be made more often than nine times a year. Therefore, we estimate that *one set of measurements for every 1 to 1.3 months annually should yield an annual mean value within the desired $\pm 6 \mu\text{atm}$ (needed for $\pm 0.1 \text{ Pg C/yr}$, see Table D-1) over the temperate North Atlantic region.*

D.4.2 Equatorial Pacific regime

The temporal variability of the sea-air pCO₂ difference (ΔpCO_2) at the Equatorial Pacific is shown from mooring data taken at 2°S and 170°W from 22 June 1998, to 3 May 2000 (Gernot Friederich and Francisco Chavez, MBARI, see Fig. D-5). The variability of surface water pCO₂ in this region is very closely associated with sea surface temperature values indicating upwelling events due to a combination of local wind events, the remnants of tropical instability waves and Kelvin waves propagated by Madden and Ju-

lian Oscillation in the atmosphere (Chavez *et al.*, 1999). The increase in $\Delta p\text{CO}_2$ over the measurement period is most likely due to the increase in upwelling as the Eastern Equatorial Pacific recovers from El-Niño conditions. Figure D-6 shows the error in the estimate of the mean from the standard error (dashed curve), randomly spaced sampling (open circles and solid line), and evenly spaced sampling (solid curve) over an annual cycle. This data set would need to be sampled ~ 30 times a year randomly or ~ 15 times a year at equal intervals to achieve an average annual $\Delta p\text{CO}_2$ of $4.4 \mu\text{atm}$ (the $\Delta p\text{CO}_2$ needed to estimate the flux of CO_2 to the nearest 0.1 Pg of C in the North Pacific, Table D-1).

D.4.3 Subarctic regime

The temporal (seasonal) variability of the surface water $p\text{CO}_2$ in an approximately $4^\circ \times 5^\circ$ area located north of Iceland is shown in Fig. D-7. The $p\text{CO}_2$ values were obtained by Jon Olafsson of MRI, Reykjavik, and the LDEO staff over the 14-year period, 1983–1997. Since no obvious interannual changes can be identified, the data in this period are plotted against a time span of 1 year, and thus the plot includes the interannual variability as well as the spatial variability within this area box. The data associated with salinity values less than 34.0 have been removed in order to eliminate the effects of low salinity arctic waters. An abrupt drawdown of surface water $p\text{CO}_2$ amounting to about $250 \mu\text{atm}$ is observed about Julian day 150, and this coincides with the formation of a well-stratified mixed layer and a rapid increase in the temperature of the mixed layer. The sudden decrease in $p\text{CO}_2$ is attributed primarily to the biological utilization of CO_2 , but is partially compensated by the concurrent increase in temperature (Takahashi *et al.*, 1993). The mean annual $p\text{CO}_2$ in surface waters is $311.3 \mu\text{atm}$ with a standard deviation of $41 \mu\text{atm}$ and a standard error in the mean of $\pm 2.4 \mu\text{atm}$ (with a total of 284 measurements).

The error for the annual mean $p\text{CO}_2$ calculated by randomly and evenly time-spaced sampling of the observation is shown in Fig. D-8 as a function of the number of sampling events per year. Based on this plot, we estimate that 5 to 8 evenly spaced observations or 8 to 15 randomly spaced observations annually should yield an annual mean value within the desired $\pm 11 \mu\text{atm}$ (needed for $\pm 0.1 \text{ Pg C/yr}$, see Table D-1) over the subarctic North Atlantic region.

D.4.4 Transition zone between the temperate and subarctic regimes

The temporal (seasonal) variability of the surface water $p\text{CO}_2$ in an approximately $4^\circ \times 5^\circ$ area that includes the Weather Station “P” in the northeastern North Pacific (50°N , 145°W) is shown in Fig. D-9. The observations were made in the 3-year period, 1972–1975, and are plotted against Julian day as though all measurements were made in one year. Therefore, the plot includes the interannual variability. Figure D-9 shows relatively small seasonal peak-to-peak amplitude of about $50 \mu\text{atm}$ (compared with

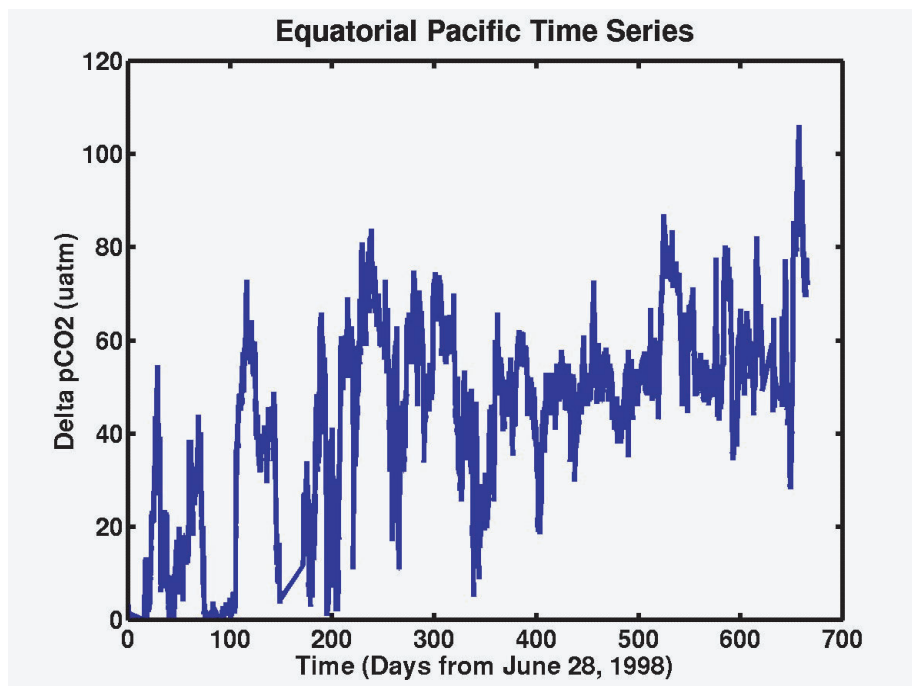


Figure D-5: Equatorial Pacific mooring measurements of $\Delta p\text{CO}_2$ taken at 2°S and 170°W from 22 June 1998, to 3 May 2000. This data was collected by Gernot Friederich and Francisco Chavez (MBARI).

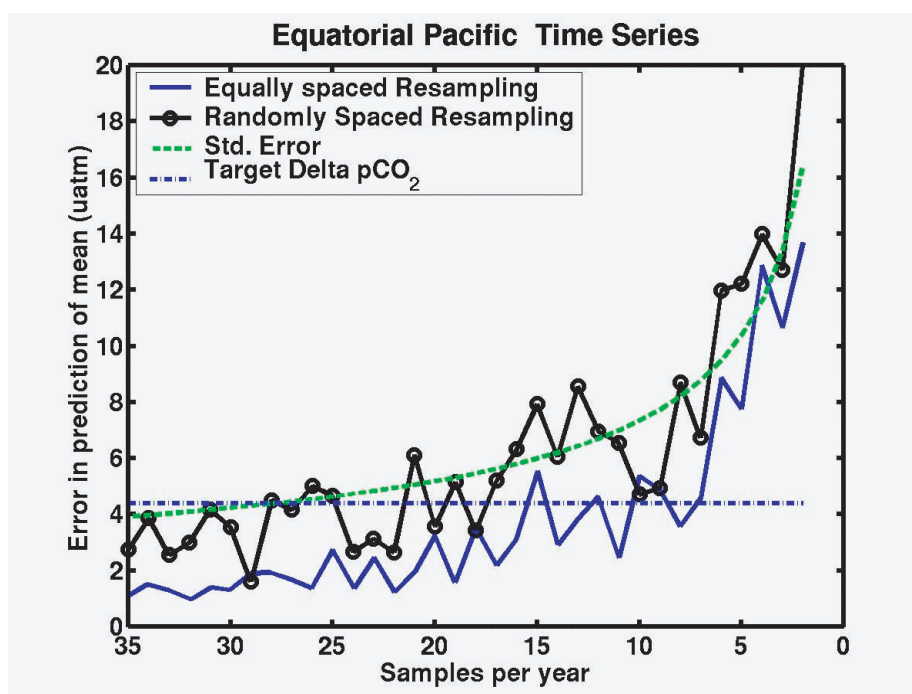


Figure D-6: Error for the annual mean value as a function of sampling frequency per year in the Equatorial Pacific at 2°S and 170°W. The standard error in the mean (dashed curve). Sampling with equal time intervals (solid curve). Sampling with randomly spaced time intervals (open circles and solid line). The dotted-dashed line refers to the $\Delta p\text{CO}_2$ needed to estimate the flux of CO₂ to the nearest 0.1 Pg of C in the Equatorial Pacific.

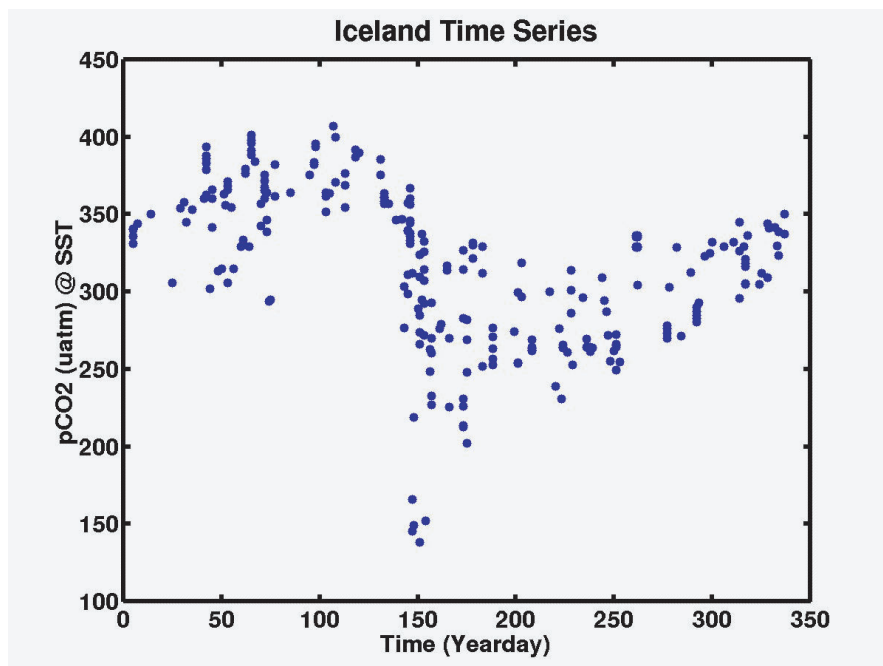


Figure D-7: The temporal (seasonal) variation of surface water pCO₂ in a 4° × 5° area located north of Iceland. The data were obtained by Jon Olafsson (MRI, Reykjavik) and the LDEO staff over the 14-year period, 1983–1997.

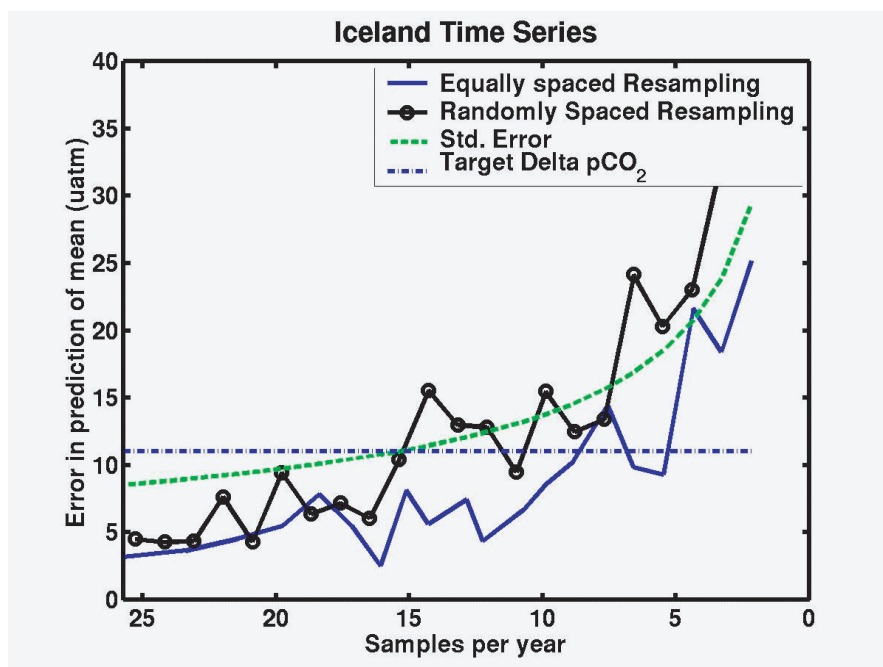


Figure D-8: Error for the annual mean value of surface pCO₂ as a function of sampling frequency per year in a 4° × 5° area located north of Iceland. The standard error in the mean (dashed curve). Sampling with equal time-intervals (solid curve). Sampling with randomly spaced time intervals (open circles and solid line). The dotted dashed line refers to the $\Delta p\text{CO}_2$ needed to estimate the flux of CO₂ to the nearest 0.1 Pg of C in the subarctic North Atlantic region.

100 μatm near Bermuda (Fig. D-3) and 250 μatm near Iceland (Fig. D-7)), and shows no simple sinusoidal seasonal patterns (like that observed near Bermuda (Fig. D-3)). This may be attributed to the fact that the seasonal temperature effect on pCO₂ is similar in amplitude but about 6 months out of phase from the biological effect (Takahashi *et al.*, 1993). While the effect of summer warming of water increases surface water pCO₂, the biological CO₂ utilization that increases toward a summer maximum reduces pCO₂, thus partially or entirely canceling each other. Large oceanic areas located along the boundary between the temperate and subpolar regimes, especially in the southern hemisphere oceans between 40°S and 60°S, also exhibit a zone of small seasonal amplitude in surface water pCO₂ (Takahashi *et al.*, submitted).

The error for the annual mean pCO₂ anticipated for measurements with evenly time-spaced sampling, is shown in Fig. D-10 as a function of the number of sampling events per year. Based on this plot, we estimate that ~ 9 evenly spaced observations or ~ 15 randomly spaced observations a year should yield an annual mean value within the desired $\pm 3 \mu\text{atm}$ (needed for $\pm 0.1 \text{ Pg C/yr}$, see Table D-1) over the temperate/subarctic North Pacific region.

D.5 Spatial Variability of CO₂ and Sampling Intervals

We have also analyzed scales of variability in the surface water pCO₂ values measured along ship's tracks using semicontinuous equilibrator-IR systems. To represent different oceanographic regimes, we have chosen (1) an E-W traverse across the temperate North Atlantic, (2) a N-S traverse across the central Pacific including the high pCO₂ equatorial zone, and (3) a pair of N-S traverses during summer and winter across the subpolar and polar regimes in the Pacific sector of the Southern Ocean. The analysis of these data sets, which cover major oceanographic regimes, should yield the basis for designing sound strategies for mapping of the surface ocean pCO₂ over the global oceans.

D.5.1 E-W traverse across the temperate North Atlantic Ocean

The spatial variability in pCO₂ for the temperate North Atlantic is illustrated using a transect from Punta Del Gado, Azores to Miami, FL (Fig. D-11A) during the GASEX 98 cruise using measurements made on the NOAA research vessel R/V *Ron Brown*. The measurements of pCO₂ were made over a 10-day period extending from 28 June 1998, to 7 July 1998, and show a steady increase in pCO₂ over the westward transect to Miami, with a peak in the Gulf Stream ($\sim 5000 \text{ km}$ from the Azores, Fig. D-11B). These data were provided by the joint collaboration of AOML and PMEL (<http://www.aoml.noaa.gov/ocd/oaces/mastermap.html>).

The large-scale change in surface water pCO₂ over the course of the

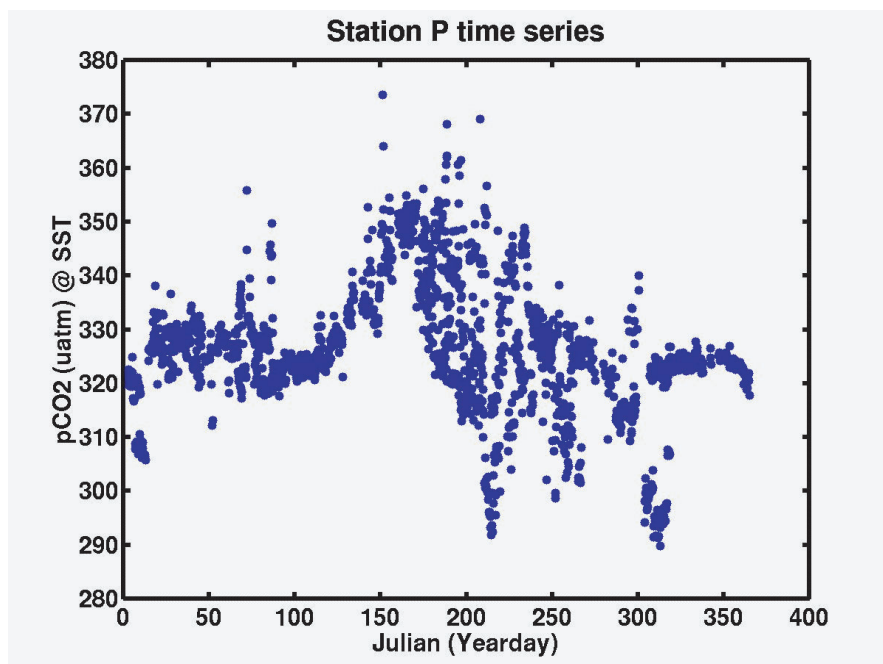


Figure D-9: Seasonal variation of surface water $p\text{CO}_2$ and SST observed at the Weather Station “P” (50°N and 145°W) by Wong and Chan (1991) in 1972–1975. Note that the SST changes more or less sinusoidal with a seasonal amplitude of 8°C , and that the surface water $p\text{CO}_2$ does not exhibit a simple sinusoidal pattern and changes only by $50 \mu\text{atm}$ (compared to $130 \mu\text{atm}$ expected from a 8°C temperature change).

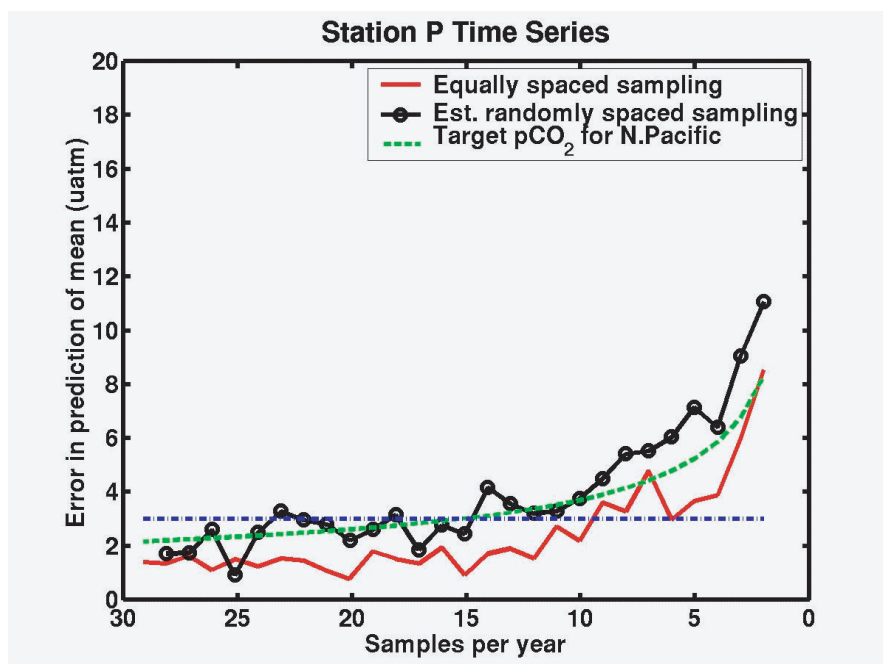


Figure D-10: Error for the annual mean value at Weather Station “P”. The standard error in the mean (dashed curve). Sampling with equal time intervals (solid curve). Sampling with randomly spaced time intervals (open circles and solid line). The dotted-dashed line refers to the $\Delta p\text{CO}_2$ needed to estimate the flux of CO_2 to the nearest 0.1 Pg of C in the temperate North Pacific.

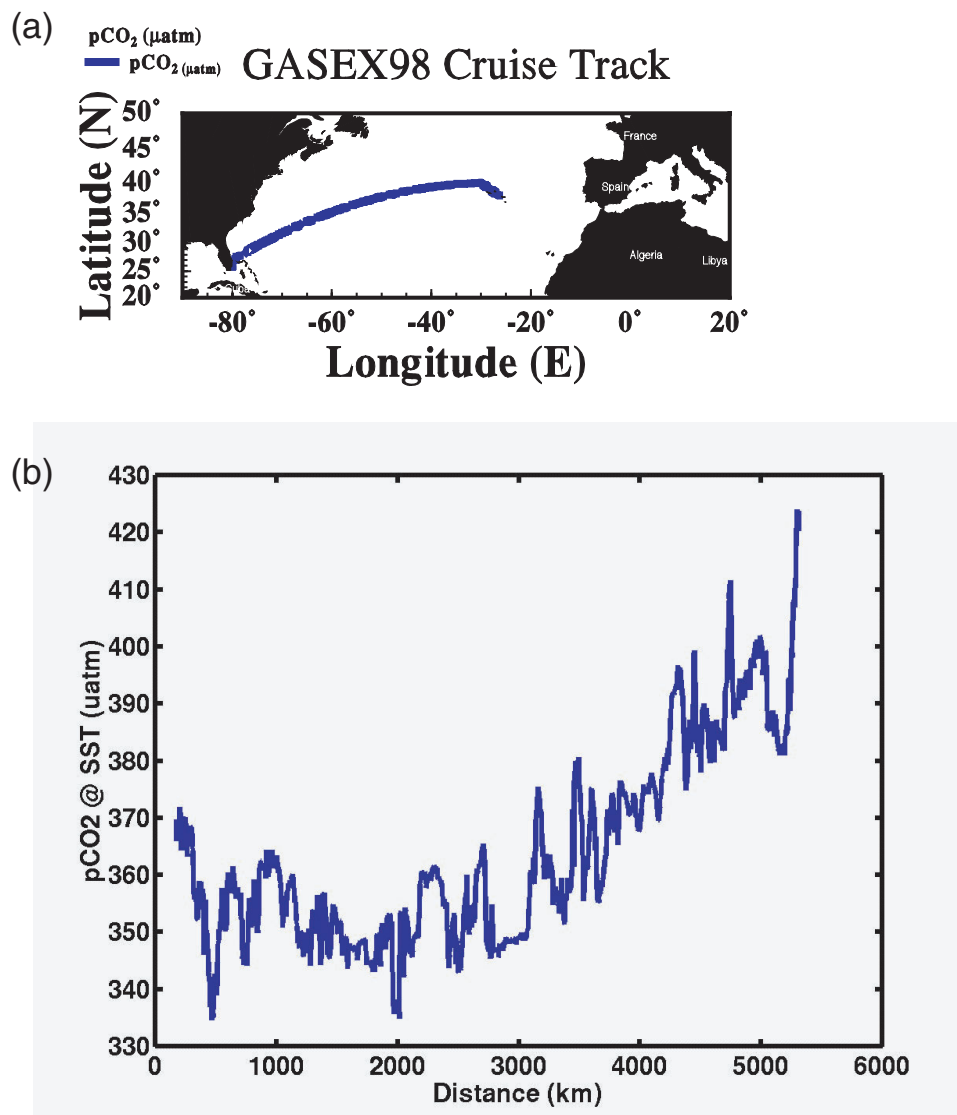


Figure D-11: (a) Cruise track of the NOAA R/V *Ron Brown* from Punta Del Gado, Azores, to Miami, FL, from 28 June 1998, to 7 July 1998, during GASEX 98. (b) Surface water $p\text{CO}_2$ as a function of the distance from Azores. These data were provided by the joint collaboration of AOML and PMEL (<http://www.aoml.noaa.gov/ocd/oaces/mastermap.html>).

transect clearly dominates the variance about the mean. When the error in the estimates of the transect mean is computed for equally spaced samples (Fig. D-12), we observe that randomly spaced samples taken every ~ 750 km and evenly spaced samples taken every 1500 km should yield an annual mean value within the desired $\pm 5.6 \mu\text{atm}$ (needed for ± 0.1 Pg C/yr, see Table D-1).

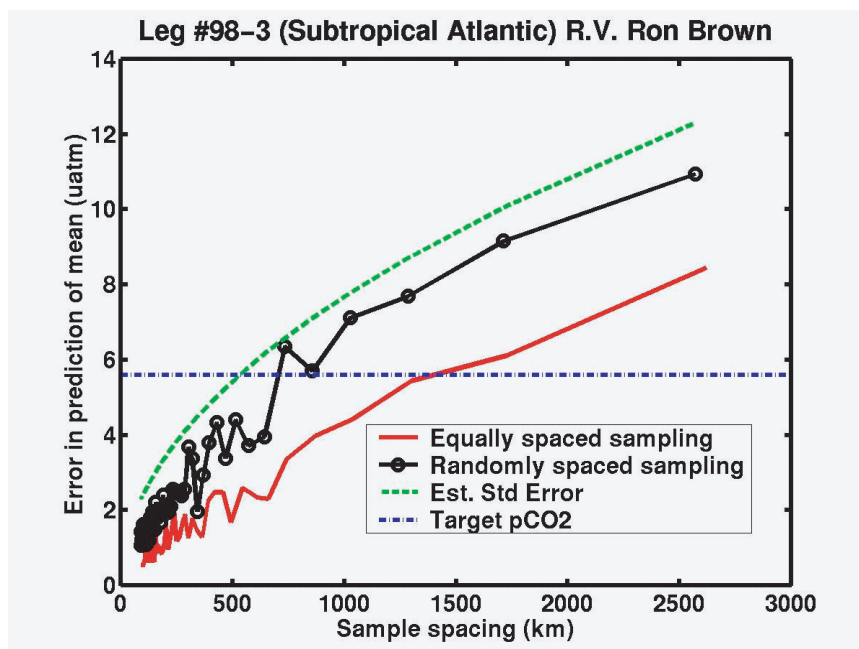


Figure D-12: Error estimate of mean surface pCO₂ during transect of the NOAA R/V *Ron Brown* from Punta Del Gado, Azores, to Miami, FL. The standard error in the mean (dashed curve). Sampling with equal time-intervals (solid curve). Sampling with randomly spaced time intervals (open circles and solid line). The dotted dashed line refers to the Δ pCO₂ needed to estimate the flux of CO₂ to the nearest 0.1 Pg of C in the temperate North Atlantic.

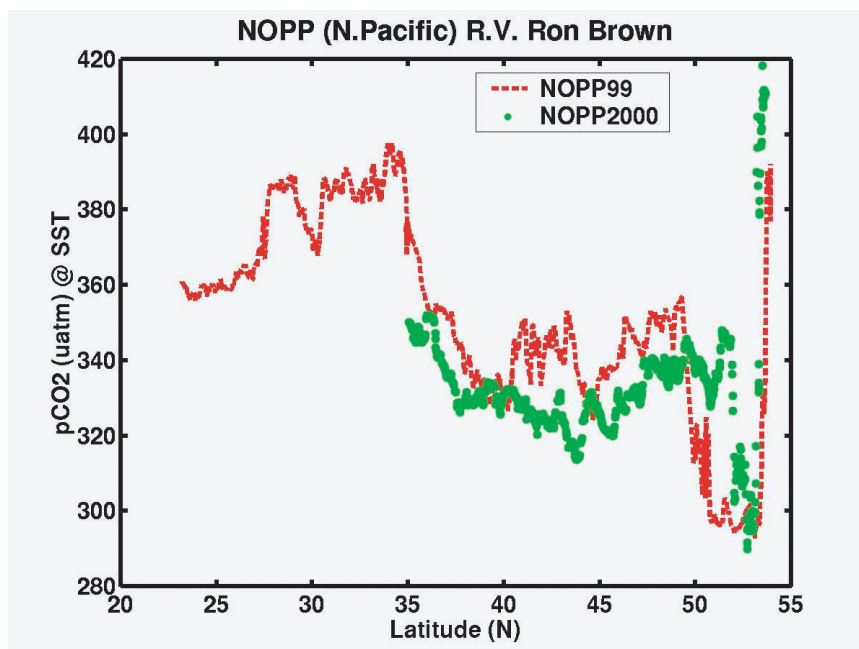


Figure D-13: Surface pCO₂ at sea surface temperature measured on the NOAA R/V *Ron Brown* from Honolulu, HI, to Dutch Harbor, AK, along the $\sim 170^\circ$ W meridian between 26 September and 3 October 1999 (NOPP99). Surface pCO₂ at sea surface temperature measured on the R/V *Ron Brown* from Dutch Harbor, AK, to San Diego, CA, during a 12-day period between 27 September and 9 October 2000 (NOPP2000). These data were provided by the joint collaboration of AOML and PMEL (<http://www.aoml.noaa.gov/ocd/oaces/mastermap.html>).

D.5.2 N-S traverse across the central north and equatorial Pacific Ocean

As in the temperate North Atlantic, the required sampling intervals to make flux estimates with errors less than 0.1 Pg C/yr requires less sampling because of a reduced level of mesoscale variability in surface pCO₂ in these areas. This is demonstrated by a transect from Honolulu, HI, to Dutch Harbor, AK, along the ~170°W meridian during an 8-day period between 26 September and 3 October 1999 (NOPP99, Fig. D-13). A similar transect is also shown from a transect that took place a year later from Dutch Harbor, AK, to San Diego, CA, during a 12-day period between 27 September and 9 October 2000 (NOPP2000, Fig. D-13). These data were provided by the joint collaboration of AOML and PMEL (<http://www.aoml.noaa.gov/ocd/oaces/mastermap.html>). Both surface pCO₂ profiles indicate strong fronts at ~34°N, ~50°N, and ~54°N where surface pCO₂ varies by as much as 60 μatm. However, between fronts the mesoscale (~100 km) variability is small. Subsampling the original datasets (Fig. D-14) indicates that evenly spaced sampling intervals of 300–700 km should yield an annual mean value within the desired ±2.9 μatm (needed for ±0.1 Pg C/yr, see Table D-1).

The spatial variability in surface pCO₂ in the temperate and northern Pacific appears to be small compared to those found in the equatorial zone (Fig. D-1). Two transects across the equator along the 95°W (eastern Pacific, the data obtained by the LDEO staff) and 170°W (central Pacific, the data provided by R.A. Feely, PMEL/NOAA) meridians show closely spaced fronts less than 200 km apart which exhibit changes in surface pCO₂ of greater than 100 μatm (Fig. D-15). A subsampling in the central and eastern Equatorial Pacific (Fig. D-16) indicates that evenly spaced sampling of 200–500 km intervals should yield an annual mean value within the desired ±4.4 μatm (needed for ±0.1 Pg C/yr, see Table D-1).

D.5.3 N-S traverses across the high-latitude Southern Ocean

The Southern Ocean exhibits the same degree of variability seen in the Pacific equatorial zone, through a combination of the ACC, strong Coriolis forcing and a large biological drawdown of CO₂, which act together to increase the mesoscale variability in this region. The effect of biology on mesoscale variability in the Southern Ocean is demonstrated by Fig. D-17, which shows two transects, one prior to the phytoplankton bloom (winter-NBP9708) and one following the phytoplankton bloom (summer-KIWI8), along ~170°W from 45°S to 63°S. It is important to note the variability north of 50°S in both transects. Variability in pCO₂ due to primary productivity during the summer months in the lower latitudes significantly affects our ability to estimate the mean by subsampling the original data set. Figure D-18 suggests that during the summer samples need to be taken every 400–800 km to get a robust estimate of the basin-scale mean value within the desired ±4.3 μatm (needed for ±0.1 Pg C/yr, see Table D-1).

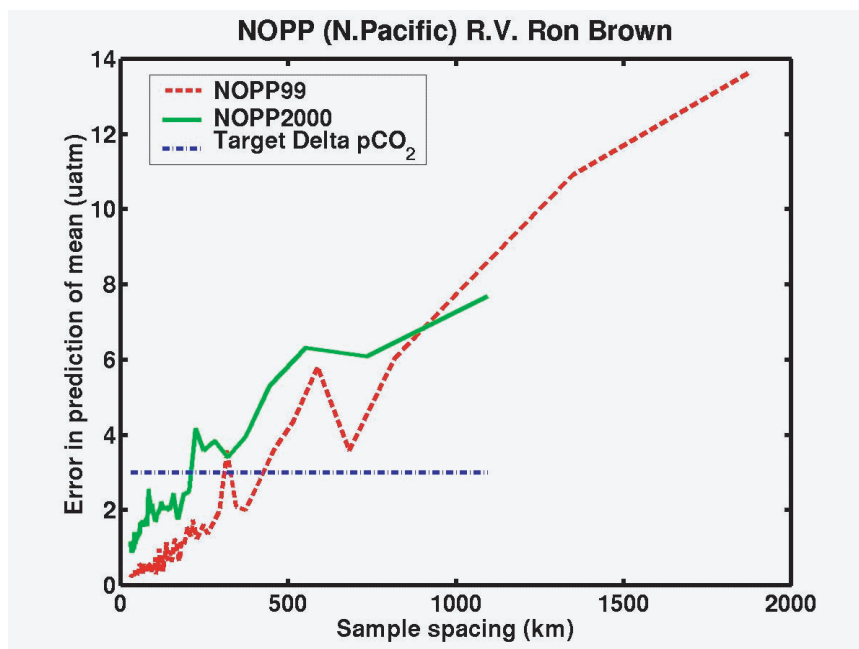


Figure D-14: Error estimate of mean surface $p\text{CO}_2$ using evenly spaced sampling intervals during the transect of the NOAA R/V *Ron Brown* from Honolulu, HI, to Dutch Harbor, AK, along the $\sim 170^\circ\text{W}$ meridian between 26 September and 3 October 1999 (NOPP99). Error estimate of mean surface $p\text{CO}_2$ using evenly spaced sampling intervals during the transect of the NOAA R/V *Ron Brown* from Dutch Harbor, AK, to San Diego, CA, during a 12-day period between 27 September and 9 October 2000 (NOPP2000). The dotted dashed line refers to the $\Delta p\text{CO}_2$ needed to estimate the flux of CO_2 to the nearest 0.1 Pg of C in the temperate North Pacific.

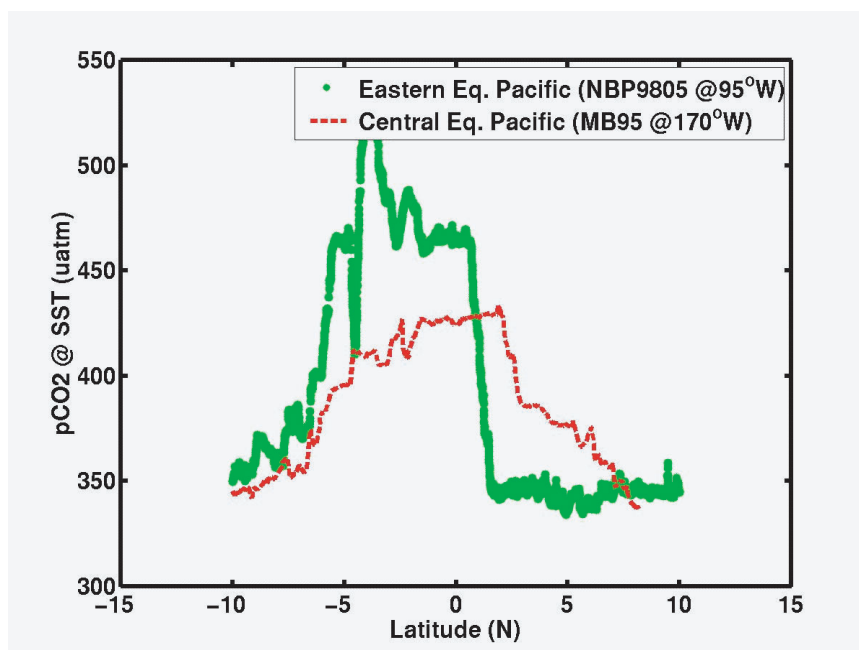


Figure D-15: Surface $p\text{CO}_2$ at sea surface temperature measured on the R/V I/B *Nathaniel B. Palmer* from Punta Arenas, Chile, to Seattle, WA, along the $\sim 95^\circ\text{W}$ meridian between 26 July and 12 August 1998 (NBP9805). Surface $p\text{CO}_2$ at sea surface temperature measured on the NOAA R/V *M. Baldrige* from Darwin, Australia to Rodman, Panama between 21 November 1995, and 17 January 1996 (MB95).

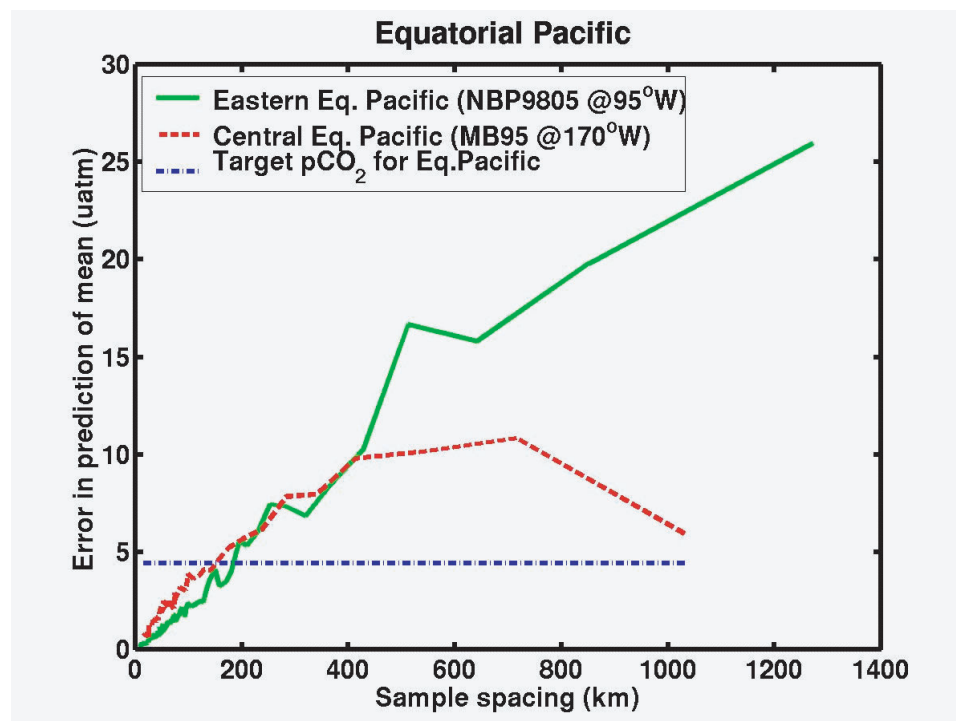


Figure D-16: Error estimate of mean surface pCO₂ using evenly spaced sampling intervals during the transect on the R/V I/B *Nathaniel B. Palmer* from Punta Arenas, Chile, to Seattle, WA, along the ~95°W meridian between 26 July and 12 August 1998 (NBP9805). Error estimate of mean surface pCO₂ using evenly spaced sampling intervals during the transect on the NOAA R/V *M. Baldrige* from Darwin, Australia, to Rodman, Panama, between 21 November 1995, and 17 January 1996 (MB95). The dotted-dashed line refers to the $\Delta p\text{CO}_2$ uncertainty needed to estimate the flux of CO₂ to the nearest 0.1 Pg of C in the Equatorial Pacific region.

D.6 Conclusion

D.6.1 Temporal and spatial sampling requirements

In the above analysis we have shown how often the sea-air pCO₂ difference in the temperate regions of North Pacific and North Atlantic need to be sampled using evenly spaced sampling to estimate regional fluxes to better than 0.1 Pg C/yr (Table D-2). In addition, we have also included the Equatorial Pacific and Southern Pacific Polar Ocean because of the high mesoscale variability in these areas. The results presented assume that the uncertainty in the estimated fluxes are due entirely to the precision of the sea-air pCO₂ difference and do not include the errors from the sea-air gas transfer coefficient. Our analysis points out that a desired uncertainty of ± 0.1 Pg C/yr in the basin-scale mean annual estimates for net sea-air CO₂ flux may be achieved by evenly time-spaced measurements of pCO₂ **6–15 times a year** throughout the regions of the world ocean with evenly spaced sampling **200–1500 km apart** (or 2–20 degrees longitude, depending on region and latitude). This analysis also points out the advantage of evenly spaced sampling in time and space over randomly spaced sampling.

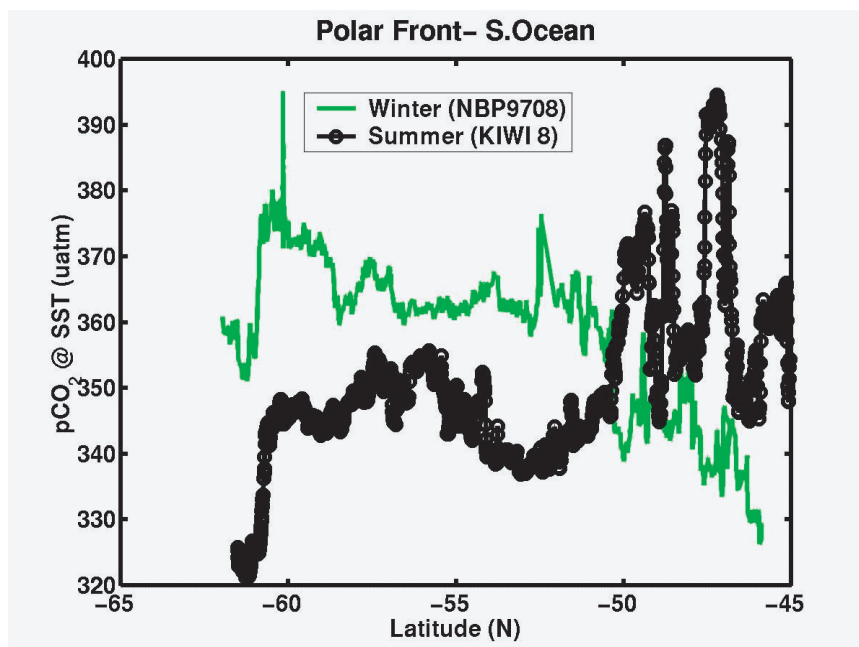


Figure D-17: Surface $p\text{CO}_2$ at sea surface temperature measured on the R/V I/B *Nathaniel B. Palmer* along $\sim 170^\circ\text{W}$ meridian between 7 and 11 November 1997 (Winter-NBP9708). Surface $p\text{CO}_2$ at sea surface temperature measured on the R/V *Revelle* along $\sim 170^\circ\text{W}$ meridian between 2 and 11 February 1998 (Summer-KIWI 8).

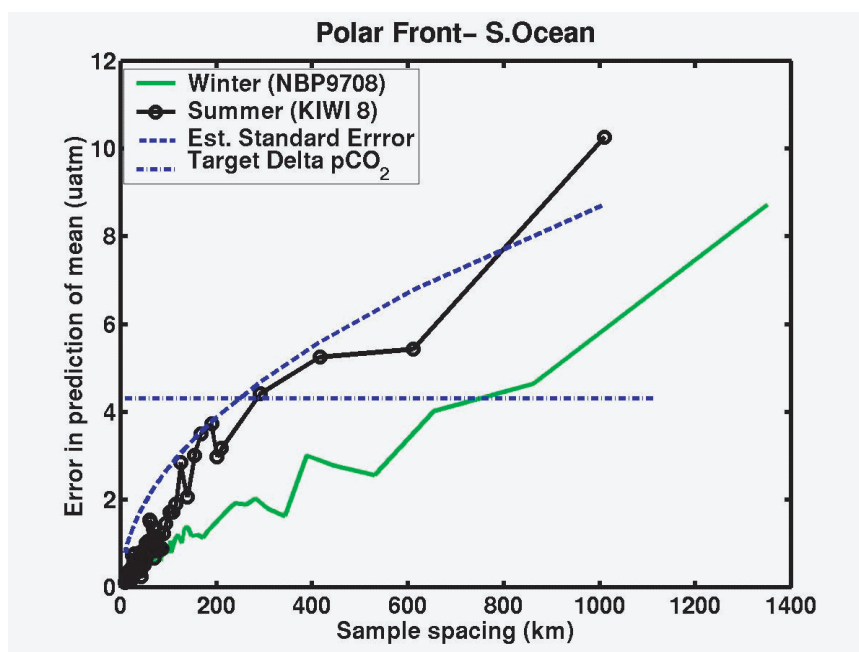


Figure D-18: Error estimate of mean surface $p\text{CO}_2$ using evenly spaced sampling intervals on the R/V I/B *Nathaniel B. Palmer* along $\sim 170^\circ\text{W}$ meridian between 7 and 11 November 1997 (Winter-NBP9708). Error estimate of mean surface $p\text{CO}_2$ using evenly spaced sampling intervals during transect on the R/V *Revelle* along $\sim 170^\circ\text{W}$ meridian between 2 and 11 February 1998 (Summer-KIWI 8). The dotted dashed line refers to the uncertainty of $\Delta p\text{CO}_2$ needed to estimate the flux of CO_2 to the nearest 0.1 Pg of C in the Polar South Pacific. The smooth dashed curve indicates the estimated standard error.

Table D-2: Mean annual sea-air pCO₂ difference, the sea-air pCO₂ required for 0.1 Pg C flux, the required evenly spaced spatial and temporal sampling needed to achieve the sea-air pCO₂*.

Region	Average	$\Delta p\text{CO}_2$	Samples	
	$\Delta p\text{CO}_2$ (μatm)	Flux = 0.1 Pg C/yr (μatm)	Spacing (km)	Samples per year
Northern North Atlantic	-47.4	10.8		~5-9
Temperate North Atlantic	-9.3	5.6	~1500	~6
Temperate North Pacific	-10.0	2.9	200-600	~9
Equatorial Pacific	29.6	4.4	200	~15
Polar South Pacific	-9.0	4.3	300-800	

*All the values are for the reference year 1995. The wind speed data of Esbensen and Kushnir (1981) and the wind speed dependence of gas transfer coefficient of Wanninkhof (1992) have been used.

In real ocean environments, wind speeds change with short timescales, and hence the sea-air CO₂ flux as the gas transfer piston velocity is affected sensitively with wind speed. Using the wind speed and pCO₂ data observed by the AOML and PMEL staff during the NOAA *Ron Brown* cruise (98-3) over the subtropical North Atlantic, we have computed the sea-air CO₂ flux using the shipboard wind speed data, and the flux data have been analyzed similarly as done for the pCO₂ data shown in Fig. D-12. While we have found on the basis of the pCO₂ data analysis that a sampling spacing of 750 km should give a precision of 0.1 Pg C in the temperate North Atlantic, an analysis of the flux data shows that about 250 km sampling spacing is needed to obtain the same precision. This suggests that the sampling spacing values evaluated in Table D-2 above represent a maximum spacing applicable to wind speeds averaged over a month rather than those averaged over a shorter time (hourly) period. We therefore recommend that surface water pCO₂ measurements be made with greater frequencies (or shorter spatial intervals) comparable to wind speed variability, so that the magnitude of the cross-correlation term for pCO₂ and wind speed variations can be evaluated.

D.6.2 Ways to lower sampling requirements

The above sampling recommendations assume that we have no prior knowledge about the spatial and temporal variability and no other proxies estimating the surface concentration of pCO₂.

Subjective sampling

Given some knowledge of the known spread of variance throughout time and space, it may be possible to improve our estimate of the mean by sampling at high resolution in spatial or temporal gradients and lower resolution in areas where the known gradients are not as steep. This subjective approach may serve to reduce the required number of samples in a given area. In order

to insure that no bias results from this approach to sampling, each region will need to be oversampled initially.

Use of proxies

The fact that we are able to predict the mean value of the sea-air pCO₂ difference with evenly spaced sampling so much better than randomly spaced sampling is directly related to the fact that the sea-air pCO₂ difference is autocorrelated. Simply stated, sequential measurements of surface pCO₂ in time and space are correlated with each other over some distance that is related to the sampling frequency that we have specified in Table D-2. Without prior knowledge of the field, it is more efficient to sample at evenly spaced intervals than randomly spaced intervals.

In addition to being autocorrelated, surface pCO₂ is also correlated with other parameters such as temperature (Stephens *et al.*, 1995) and chlorophyll concentrations, which can be observed remotely using instruments like the Pathfinder AVHRR for sea surface temperature and SeaWiFS for ocean color and biological productivity estimates. By building regionally specific algorithms to take advantage of these correlations we should be able to further decrease samples needed to predict the mean surface water pCO₂ for both regional and annual estimates.

While it is clear from this analysis that the mean surface water pCO₂ is driven primarily by large-scale variability in the ocean (>300 km), it is important that mesoscale processes not be disregarded. Multiparameter observations of mesoscale processes using moorings and high-resolution underway sampling techniques will be essential to understanding the processes that are responsible for the statistical covariance observed. It is therefore important to design a sea-air CO₂ flux program that combines the regional scale surface ocean pCO₂ observations with an ample dose of relevant process studies.

D.7 References

- Chavez, F.P., P.G. Strutton, G.E. Friederich, R.A. Feely, G.A. Feldman, D. Foley, and M.J. McPhaden (1999): Biological and chemical response of the equatorial Pacific Ocean to the 1997 and 1998 El Niño. *Science*, 286, 2126–2131.
- Esbensen, S.K., and Y. Kushnir (1981): The heat budget of the global ocean: An atlas based on estimates from the surface marine observations. *Climatic Research Institute Report #29*, Oregon State University, Corvallis, OR.
- Stephens, M.P., G. Samuels, D.B. Olson, R.A. Fine, and T. Takahashi (1995): Sea-air flux of CO₂ in the North Pacific using shipboard and satellite data. *J. Geophys. Res.*, 100, 13,571–13,583.
- Takahashi, T., J. Olafsson, J. Goddard, D.W. Chipman, and S.C. Sutherland (1993): Seasonal variation of CO₂ and nutrients in the high-latitude surface oceans: A comparative study. *Global Biogeochem. Cycles*, 7, 843–878.
- Takahashi, T., R.A. Feely, R. Weiss, R.H. Wanninkhof, D.W. Chipman, S.C. Sutherland, and T.T. Takahashi (1997): Global air-sea flux of CO₂: an estimate based on measurements of sea-air pCO₂ difference. *Proc. Natl. Acad. Sci.*, 94, 8292–8299.
- Takahashi, T., R.H. Wanninkhof, R.A. Feely, R.F. Weiss, D.W. Chipman, N. Bates, J. Olafsson, C. Sabine, and S.C. Sutherland (1999): Net sea-air CO₂ flux over

- the global oceans: An improved estimate based on the sea-air pCO₂ difference. In *Proceedings of the 2nd International Symposium, CO₂ in the Oceans* (ISSN 1341-4356), Yukihiro Nojiri (ed.), Center for Global Environmental Research, National Institute for Environmental Studies, Tsukuba, Japan, 9–14.
- Takahashi, T., S.C. Sutherland, C. Sweeney, A. Poisson, N. Metzl, B. Tilbrook, N. Bates, R. Wanninkhof, R.A. Feely, C. Sabine, and J. Olafsson, Biological and temperature effects on seasonal changes of pCO₂ in global ocean surface waters, submitted to *Deep-Sea Research*.
- Wanninkhof, R. (1992): Relationship between wind speed and gas exchange. *J. Geophys. Res.*, *97*, 7373–7382.
- Wanninkhof, R., and W.R. McGillis (1999): A cubic relationship between air-sea CO₂ exchange and wind speed. *Geophys. Res. Lett.*, *26(13)*, 1889–1892.
- Wong, C.S., and Y.-H. Chan (1991): Temporal variations in the partial pressure and flux of CO₂ at ocean station P in the subarctic northeast Pacific Ocean. *Tellus*, *43B*, 206–223.